

# Accepted Manuscript

Design, Synthesis and Biological Activity of 3-Pyrazine-4-yl-oxazolidin-2-ones as Novel, Potent and Selective Inhibitors of Mutant Isocitrate Dehydrogenase 1

Tianfang Ma, Fangxia Zou, Stefan Pusch, Lijun Yang, Qihua Zhu, Yungen Xu, Yueqing Gu, Andreas von Deimling, Xiaoming Zha

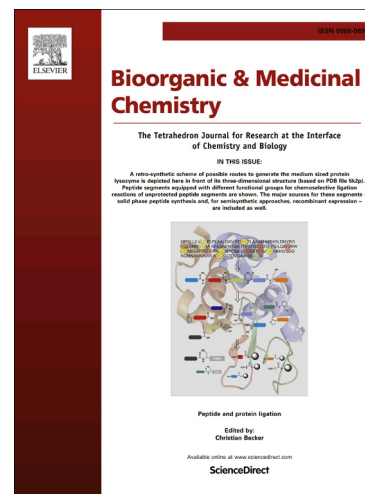
PII: S0968-0896(17)31543-2  
DOI: <https://doi.org/10.1016/j.bmc.2017.10.009>  
Reference: BMC 14014

To appear in: *Bioorganic & Medicinal Chemistry*

Received Date: 29 July 2017  
Revised Date: 8 October 2017  
Accepted Date: 12 October 2017

Please cite this article as: Ma, T., Zou, F., Pusch, S., Yang, L., Zhu, Q., Xu, Y., Gu, Y., von Deimling, A., Zha, X., Design, Synthesis and Biological Activity of 3-Pyrazine-4-yl-oxazolidin-2-ones as Novel, Potent and Selective Inhibitors of Mutant Isocitrate Dehydrogenase 1, *Bioorganic & Medicinal Chemistry* (2017), doi: <https://doi.org/10.1016/j.bmc.2017.10.009>

This is a PDF file of an unedited manuscript that has been accepted for publication. As a service to our customers we are providing this early version of the manuscript. The manuscript will undergo copyediting, typesetting, and review of the resulting proof before it is published in its final form. Please note that during the production process errors may be discovered which could affect the content, and all legal disclaimers that apply to the journal pertain.



# Design, Synthesis and Biological Activity of 3-Pyrazine-4-yl-oxazolidin-2-ones as Novel, Potent and Selective Inhibitors of Mutant Isocitrate Dehydrogenase

## 1

Tianfang Ma<sup>a,b,#</sup>, Fangxia Zou<sup>a,b,#</sup>, Stefan Pusch<sup>c,d,#</sup>, Lijun Yang<sup>a,b</sup>, Qihua Zhu<sup>b</sup>, Yungen Xu<sup>b</sup>,

Yueqing Gu<sup>a</sup>, Andreas von Deimling<sup>c,d,\*</sup>, Xiaoming Zha<sup>a,b,\*</sup>

<sup>a</sup> Department of Pharmaceutical Engineering & Department of Biochemical Engineering, China Pharmaceutical University, 639 Longmian Avenue, Nanjing 211198, China.

<sup>b</sup> Department of Medicinal Chemistry, China Pharmaceutical University, 24 Tongji Xiang, Nanjing 210009, PR China.

<sup>c</sup> German Consortium of Translational Cancer Research (DKTK), Clinical Cooperation Unit Neuropathology, German Cancer Research Center (DKFZ), INF 280, Heidelberg D-69120, Germany.

<sup>d</sup> Department of Neuropathology, Institute of Pathology, INF 224, Ruprecht-Karls-University Heidelberg, Heidelberg D-69120, Germany.

**ABSTRACT:** Isocitrate dehydrogenases (IDHs) catalyze the oxidative decarboxylation of isocitrate to alpha-ketoglutarate ( $\alpha$ -KG) generating carbon dioxide and NADPH/NADH. Evidence suggests that the specific mutations in IDH1 are critical to the growth and reproduction of some tumor cells such as gliomas and acute myeloid leukemia, emerging as an attractive antitumor target. In order to discover potent new mutant IDH1 inhibitors, we designed, synthesized and evaluated a series of allosteric mIDH1 inhibitors harboring the scaffold of 3-pyrazine-4-yl-oxazolidin-2-ones. All tested compounds

effectively suppress the D-2-hydroxyglutarate (D-2-HG) production in cells transfected with IDH1-R132H and IDH1-R132C mutations at 10  $\mu$ M and 50  $\mu$ M. Importantly, compound **3g** owns the similar inhibitory activity to the positive agent **NI-1** and shows no significant toxicity at the two concentrations. The parallel artificial membrane permeation assay of the blood-brain barrier (PAMPA-BBB) identified **3g** with a good ability to penetrate the blood-brain barrier (BBB). These findings indicate that **3g** deserves further optimization as a lead compound for the treatment of patients with IDH1 mutated brain cancers.

**Key words:** Mutant IDH1; inhibitors; D-2-HG; allosteric; BBB.

## 1. Introduction

Isocitrate dehydrogenases (IDHs), a key enzyme family associated with the tricarboxylic acid (TCA), catalyze oxidative decarboxylation of isocitrate acid to  $\alpha$ -ketoglutaric ( $\alpha$ -KG) using divalent magnesium ion and NADP<sup>+</sup> (or NAD<sup>+</sup>) as cofactors, which is critical to biosynthesis and energy metabolism [1]. Isocitrate dehydrogenase 1 (IDH1), one of the IDHs, locates in the cytosol and peroxisome, while IDH2 and IDH3 in mitochondria. IDH1 is the only NADPH producer in the biosynthesis and the thiolated antioxidant system and plays a vital role in the process of adipogenesis and phospholipid metabolism [2].

Recent studies revealed that IDH1 is a metabolic enzyme associated with the progression of cancers, and mutant IDH1 (mIDH1) primarily exists in gliomas, acute myeloid leukemia and other solid tumors [3,4]. Substantial data suggests that more than 70% low-grade gliomas and up to 20% secondary glioblastoma multiform are related to IDH1 mutations [5]. In addition, mutant IDH1 is also found in about 10% of AML cases and 10% of cholangiocarcinomas, as well as melanomas and chondrosarcomas

[5]. The most common mutation in IDH1 is a key amino acid residue Arg132 located in the active site, in which R132H is the predominant [6].

Mutations in IDH1 are heterozygous missense mutations which lead to an arginine at amino acid 132 replaced by different amino acid residues, including R132H, R132C, R132L, R132G, R132S and R132W [2]. mIDH1 exhibits a neomorphic catalytic activity to catalyze the conversion of  $\alpha$ -KG to D-2-hydroxyglutarate (D-2-HG) [7]. Comparably, IDH1 mutated cells show higher concentrations of D-2-HG than normal cells, which can be as a significant evaluation of certain tumors. D-2-HG, an oncometabolite related to tumorigenesis, induces hypermethylation of histone and chromatin and blocks cell differentiation through competitive inhibition with relevant  $\alpha$ -KG-dependent dioxygenases, such as methylases and histone demethylases [8,9]. Therefore, high level of D-2-HG from IDH1 mutations are sufficient to promote the initiation and progression of cancers, such as gliomas and acute myeloid leukemia [10]. Taken these findings into consideration, it is demonstrated that potent drugs targeting mutant IDH1 should be developed for the treatment of IDH1 mutated tumors, including brain tumors.

To date, a number of mutant IDH1 inhibitors have been reported and only **IDH-305** (structure not disclosed), **FT-2102** (structure not disclosed), **BAY-1436032** and **AG-120** have entered into clinical trials, of which **AG-120** in Phase III clinical trial [11,12]. According to the binding modes, the active sites of mIDH1 inhibitors could be classified as four types: substrate-based pocket, Seg-2 allosteric pocket,  $Mg^{2+}$  pocket and other type. **SYC-435 (1)**, a representative agent based on substrate-based pocket ( $K_i = 120$  nM), reveals a significant selectivity for mIDH1 over WT-IDH1 [13]. **GSK321 (2)**, binding to the Seg-2 allosteric pocket and locking the mutant proteins into a catalytically inactive “open” conformation to prevent mIDH1 turnover, inhibits the D-2-HG production and the growth and differentiation of mIDH1 cells [14,15]. **VVS (3)**, with  $IC_{50}$  values of 11 nM against IDH1-R132H and

259 nM against IDH1-R132C, is noncompetitive with NADPH and can selectively inhibit mIDH1 via direct interaction with Asp279 in the metal-binding pocket [16]. **AGI-5198 (4)**, developed by Agios Pharmaceuticals, is a potent and selective mIDH1 inhibitor that reduces levels of D-2-HG in tumor cells with the  $IC_{50}$  values of 70 nM and 160 nM against IDH1-R132H and IDH1-R132C, respectively [17,18]. **AG-120 (5)**,  $IC_{50} = 8$  nM) is under a Phase III clinical trial and early evidence suggested it is well tolerated with majority of mild to moderate adverse events [11,12]. **BAY-1436032 (6)** is a novel pan-inhibitor of IDH1 with different codon 132 mutations [19]. Recently, it has been entered into Phase I to evaluate its safety, tolerability, pharmacokinetics, and pharmacodynamics in patients with IDH1-R132 mutated tumors [20,21]. **BRD-2879 (7)** and **8**, discovered by high-throughput screen (HTS) and further optimization, are potent and selective mIDH1 inhibitors [22,23]. Notably, Novartis reported a novel class of mIDH1 inhibitors with 3-pyrimidin-4-yl-oxazolidin-2-ones motif, such as **NI-1 (9)**,  $IC_{50} = 0.094$   $\mu$ M, IDH1-R132H) [24]. In this article, to obtain more active and drug-like compounds with new scaffolds, we used **NI-1** as a template compound and designed a series of 3-pyrazine-4-yl-oxazolidin-2-ones. Interestingly, during the period of biological evaluation of our target compounds, **IDH889 (10)**,  $IC_{50} = 20$  nM), an analog of **NI-1**, was reported its co-crystal complex with IDH1-132H [25]. The disclosed structures of **1-10** are presented (Fig. 1).

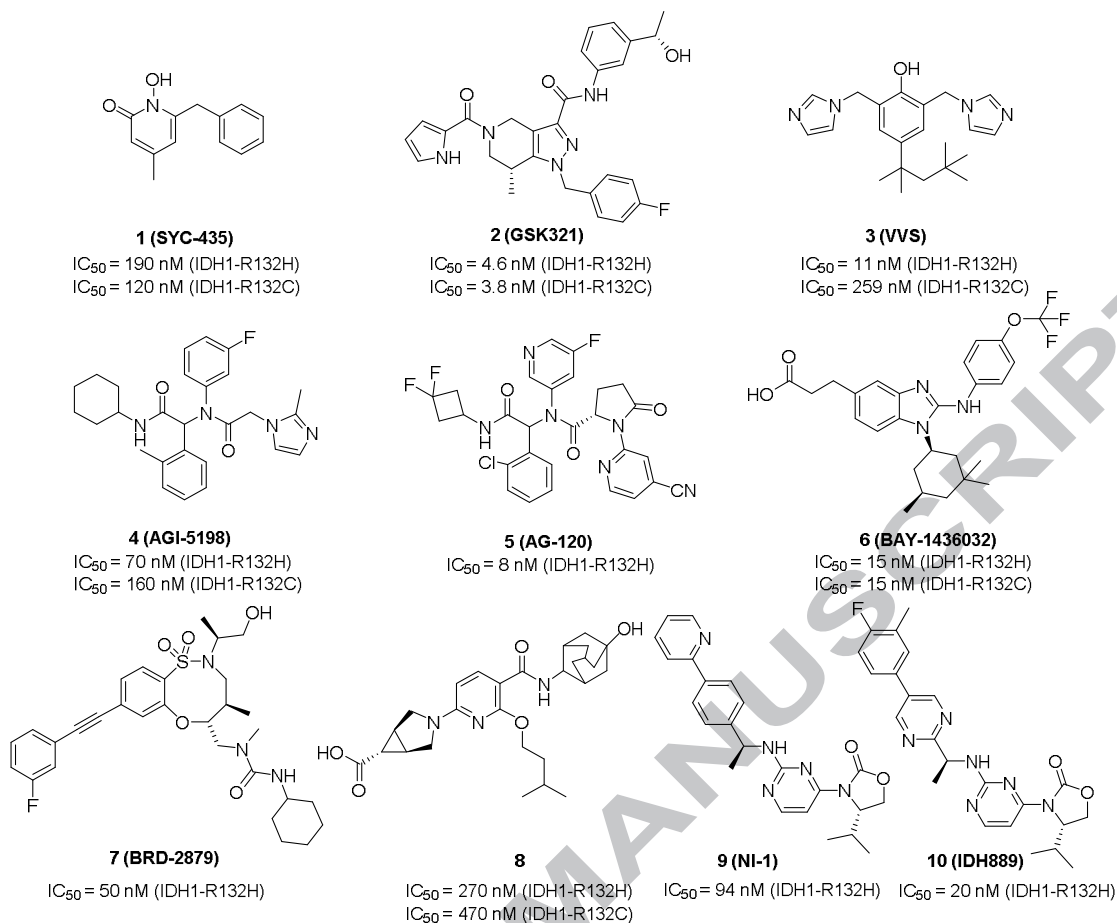


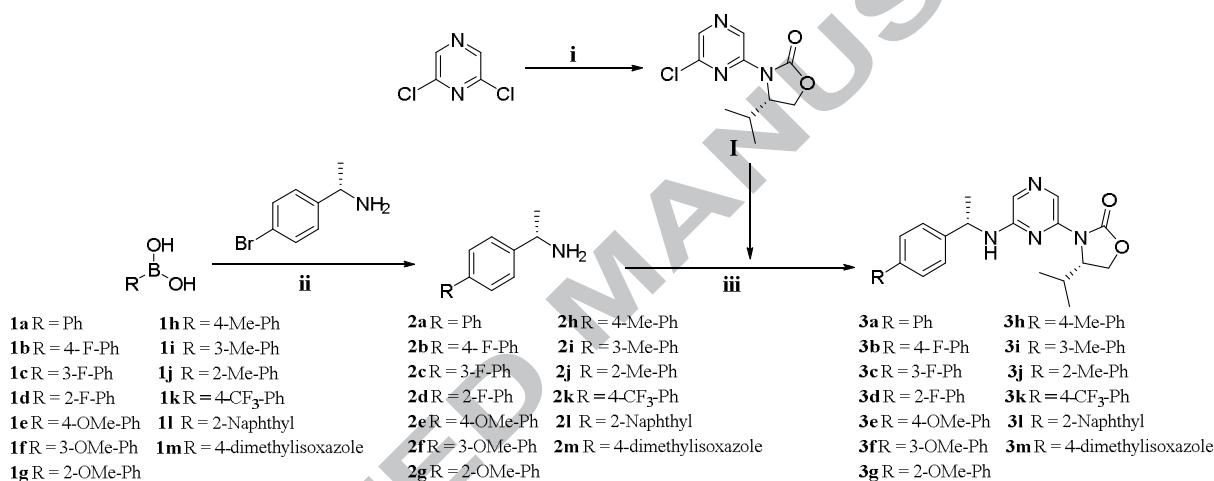
Fig. 1. Representative structures of reported mIDH1 inhibitors.

Based on the analysis of these findings, we successfully designed and synthesized a series of 3-pyrazine-4-yl-oxazolidin-2-ones allosteric mIDH1 inhibitors. All compounds display inhibitory activity against D-2-HG production in tumor cells harboring IDH1-R132H and IDH1-R132C at 10  $\mu$ M and 50  $\mu$ M. The most active one **3g** displays weak inhibition against WT-IDH1, indicating its good selectivity for mIDH1 inhibition. Molecular docking was also studied to predict the binding mode of **3g** at the allosteric site of mIDH1. Importantly, **3g** can effectively cross BBB in PAMPA model. Taken together, our work identified 3-pyrazine-4-yl-oxazolidin-2-ones as a novel class of selective and potent allosteric mIDH1 inhibitors, and **3g** deserves further optimization as an antitumor agent to treat patients with IDH1 mutated brain cancers.

## 2. Results and Discussion

### 2.1. Chemistry.

The general route for the synthesis of the target compounds **3a-3m** is depicted in **Schemes 1**. It started from 2,6-dichloropyrazine, selectively substituted by (S)-4-isopropylloxazolidin-2-one at an ice bath to afford the intermediate **I**. (S)-1-(4-bromophenyl)ethan-1-amine was reacted with **1a-1m** under Pd[P(Ph)<sub>3</sub>]<sub>4</sub>/K<sub>2</sub>CO<sub>3</sub> at 80°C to afford the intermediates **2a-2m**. Then **I** was reacted with **2a-2m** using tris(dibenzylideneacetone)dipalladium and BINAP as the catalysts in anhydrous toluene at 90°C under nitrogen to give the target compounds **3a-3m**.



**Scheme 1.** Synthesis of target compounds **3a-3m**. Reagents and conditions: (i) (S)-4-isopropylloxazolidin-2-one, NaH, DMF, ice bath, 2h; (ii) (S)-1-(4-bromophenyl)ethan-1-amine, Pd[P(Ph)<sub>3</sub>]<sub>4</sub>, 2N K<sub>2</sub>CO<sub>3</sub> solution, MeCN, reflux, overnight; (iii) tris(dibenzylideneacetone)dipalladium, BINAP, K<sub>2</sub>CO<sub>3</sub>, toluene, reflux, overnight.

### 2.2. Biological Evaluation

**Effects of 3a-3m on D-2-HG production in HEK-293T cells expressing IDH1-R132H and IDH1-R132C.** First, we employed HEK-293T cell lines expressing IDH1-R132H and IDH1-R132C to

test the inhibitory effects of **3a-3m** at two concentrations (10  $\mu$ M and 50  $\mu$ M). **NI-1**, a known mIDH1 inhibitor, was chosen as a positive control. Then the D-2-HG concentration in the cells was measured after 3 days of incubation (Table 1). To our surprise, all the tested compounds could inhibit the D-2-HG production in cells carrying IDH1-R132H or IDH1-R132C at 50  $\mu$ M (Fig. 2). **3b**, **3g**, **3j** and **3k** showed relatively strong inhibitory effects at both 10  $\mu$ M and 50  $\mu$ M. However, **3c**, **3d**, **3f**, **3h** and **3l** exhibited relatively weak inhibitory effects on the production of D-2-HG at 10  $\mu$ M. As with **NI-1**, **3g** and **3k** strongly reduced the D-2-HG levels in the cells than other tested compounds at the two concentrations, demonstrating that the compounds with 3-pyrazine-4-yl-oxazolidin-2-ones have a bit better inhibitory effects on mutant IDH1 and deserve further optimization.

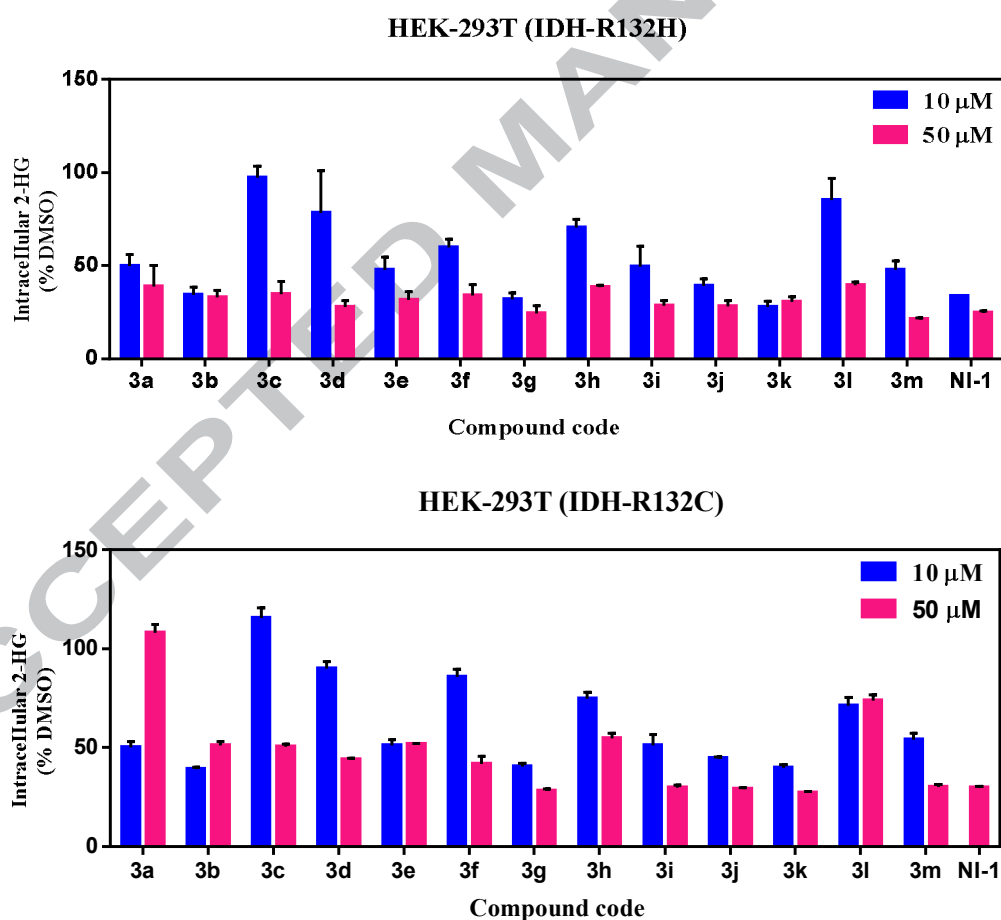
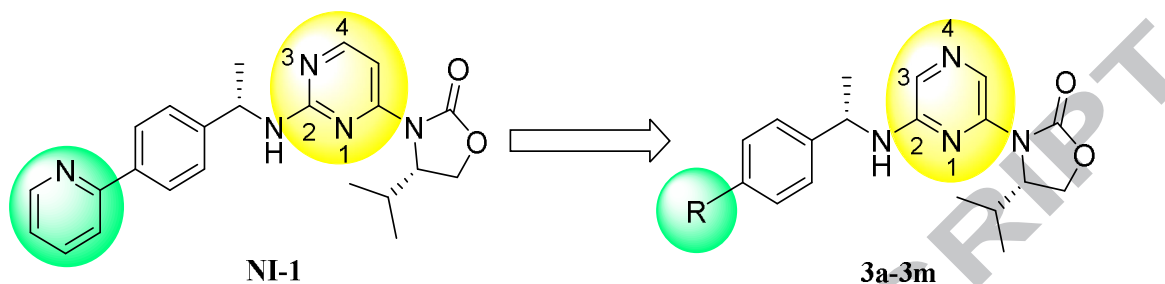


Fig. 2. The inhibitory activities of **3a-3m** and **NI-1** against IDH1-R132H and IDH1-R132C

**Table 1.** Structures and LogPs of **3a-3m** and their inhibitory effect at 10  $\mu$ M and 50  $\mu$ M in HEK-293T cells transfected with IDH1-R132H and IDH1-R132C.



Compd	R	D2HG levels (%, IDH1 R132H)		D2HG levels (%, IDH1 R132C)		LogP <sup>a</sup>
		10 $\mu$ M	50 $\mu$ M	10 $\mu$ M	50 $\mu$ M	
<b>3a</b>	Ph	50.0	38.8	50.4	108.0	4.38
<b>3b</b>	4-F-Ph	34.3	33.0	39.0	51.3	4.39
<b>3c</b>	3-F-Ph	97.2	34.7	115.5	50.6	4.37
<b>3d</b>	2-F-Ph	78.4	28.0	89.9	44.1	4.48
<b>3e</b>	4-OMe-Ph	47.7	31.9	51.3	51.7	4.43
<b>3f</b>	3-OMe-Ph	59.8	33.9	86.0	41.7	4.41
<b>3g</b>	2-OMe-Ph	31.9	24.6	40.6	28.2	4.40
<b>3h</b>	4-Me-Ph	70.5	38.7	74.9	54.8	4.63
<b>3i</b>	3-Me-Ph	49.7	28.5	51.1	29.7	4.62
<b>3j</b>	2-Me-Ph	39.2	28.3	44.6	29.1	4.61
<b>3k</b>	4-CF <sub>3</sub> -Ph	28.0	30.7	39.9	27.4	5.01
<b>3l</b>	2-naphthyl	85.4	39.5	71.3	73.9	5.27
<b>3m</b>	4-dimethylisoxazole	47.9	21.5	54.1	30.2	4.25
<b>NI-1<sup>b</sup></b>	2-pyridine	33.9	24.7	/	29.7	3.71

<sup>a</sup> LogP values were predicted at <http://www.vcclab.org/>.

<sup>b</sup> **NI-1** as a positive control.

**Cytotoxicity towards HEK-293T WT-IDH1.** Owing weak or no effects on WT-IDH1 is essential for an ideal mIDH1 inhibitor. Thus, all the compounds were tested to verify the selectivity of mIDH1 over WT-IDH1. Unexpectedly, **3b**, **3k** and **3m** exhibited relatively strong toxicity compared to other tested compounds at 50  $\mu\text{M}$ . However, **3a** and **3h** were found to retain a better selectivity between mIDH1 and wt-IDH1 at 10  $\mu\text{M}$  and 50  $\mu\text{M}$ . Importantly, **3g** had a controlled toxicity with the values of 89.8% at 10  $\mu\text{M}$  and 74.5% at 50  $\mu\text{M}$ . All the compounds showed no significant toxicity at 10  $\mu\text{M}$  (Fig. 3).

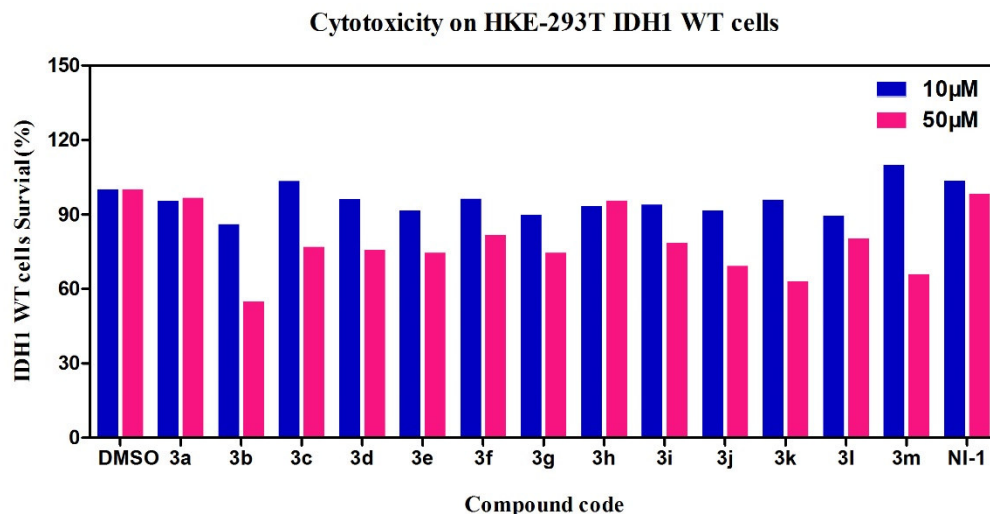


Fig. 3. Cytotoxicity of all tested compounds at 10  $\mu\text{M}$  and 50  $\mu\text{M}$  in HEK-293T WT-IDH1 cells.

**PAMPA-BBB assays.** Blood-brain barrier (BBB) permeability is essential for successful central nervous system (CNS) drugs. To measure the possible BBB permeability of **3g** *in vivo*, the parallel artificial membrane permeation assay of the blood-brain barrier (PAMPA-BBB) was performed. On the basis of the measured permeability, **3g** could cross the BBB (Table 2).

**Table 2.** Permeability ( $P_e$ ,  $\times 10^{-6}$  cm/s) results in the PAMPA-BBB assay for **3g** and its predictive penetration in the CNS.

Compd	$P_e (\times 10^{-6} \text{ cm/s})^a$	Prediction <sup>b</sup>
<b>3g</b>	$6.65 \pm 0.42$	CNS+
<b>Desipramine</b>	$8.82 \pm 0.29$	CNS+
<b>Atenolol</b>	$0.49 \pm 0.15$	CNS-

<sup>a</sup> Values are expressed as the mean  $\pm$  SD of three independent experiments. <sup>b</sup> Standards of test results are described as follows: i) CNS+ (high BBB permeation predicted):  $Pe > 4.0$ ; ii) CNS- (low BBB permeation predicted):  $Pe < 2.0$ ; iii) CNS+/- (BBB permeation uncertain):  $Pe = 2.0 \sim 4.0$ .

### 2.3. The preliminary structure-activity relationship (SAR) analysis.

As shown in Table 1, when R group is the phenyl ring, different substituents are introduced in all positions of R, which has a significant effect on the inhibitory activities of the compounds. For the para-position, **3b** (with -F) and **3k** (with  $-\text{CF}_3$ ) perform much better, while for meta- and ortho-position, **3g** (with  $-\text{OCH}_3$ ) and **3i-3j** (with  $-\text{CH}_3$ ) have better inhibitory activities, suggesting that electron-withdrawing groups in the para-position or electron-donating substituents in the meta- and ortho-position are more favorable for R. For the effects of R group's size on the activity, **3m** and **3a** exhibits relatively stronger reduction of D-2-HG levels compared to **3l**, indicating that smaller groups are more suitable for R, but larger groups are limited in this cavity.

### 2.4. Docking analysis of potential binding modes of **3g** and **NI-1**.

To understand the binding mode of the most active compound **3g** in this newly reported allosteric pocket, optimal molecular docking (CDOCKER, Discovery Studio 3.0) was performed. The C2-amine group of **3g** forms a donor-acceptor polar interaction with Ile128 and a hydrogen bond interaction is observed between the carbonyl of the oxazolidinone and the amine of Leu120. The alpha-methyl fits into a specific cavity. In addition, the isopropyl and the phenyl ring of the amine side chain are in a

hydrophobic cavity. From the superimposed complex conformation between **3g** and **NI-1**, we find that the molecular stretching direction of **3g** and **NI-1** is identical. However, 4-N of the pyrazine of **3g** can't interact with Ile128 to form a hydrogen bond. This may be the reason why **3g** shows decreased inhibitory activity compared to **NI-1** (Fig. 4).

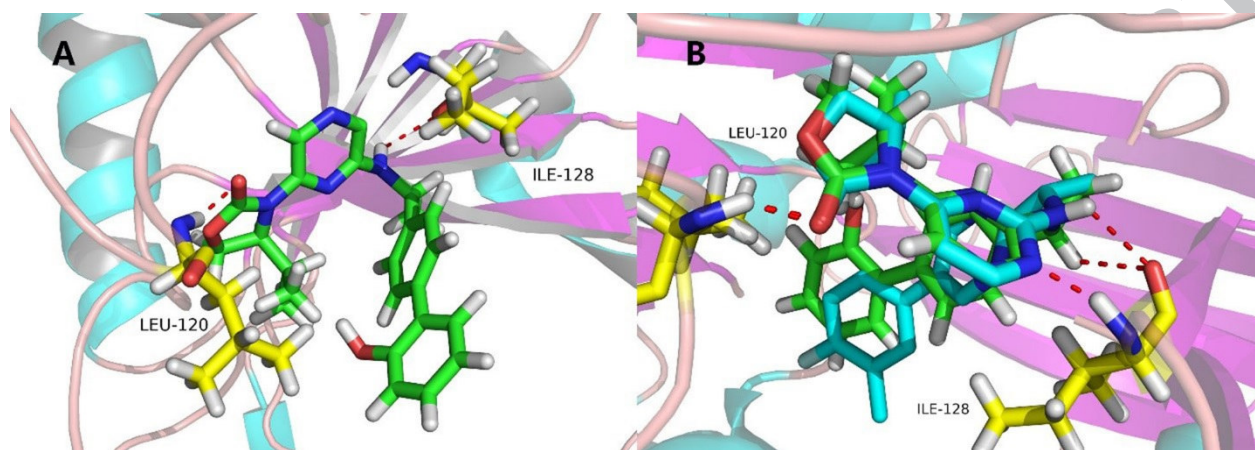


Fig. 4. Representation of the binding modes of **3g** (A) and the molecular overlap of **3g** and **NI-1** (B) with mIDH1 (PDB code: 5TQH). Key residues in yellow and the hydrogen bonds in dashed red lines.

### 3. Conclusion

In conclusion, a novel series of 3-pyrazine-4-yl-oxazolidin-2-ones as allosteric mIDH1 inhibitors were synthesized. Most of the test compounds exhibit selectivity and inhibitory effects on HEK293 cell lines harboring IDH1-R132H and IDH1-R132C and among which, **3g** is the most potent one. The molecular docking study illustrates its potential allosteric binding mode. Furthermore, **3g** also owns the ability to penetrate BBB which is of great importance for CNS drugs. Our study provides preliminary data that 3-pyrazine-4-yl-oxazolidin-2-ones may be beneficial to the design of potent and selective mIDH1 inhibitors, and the encouraging compound **3g** deserves further optimization as a lead compound to find more low-toxic and potent allosteric inhibitors for the IDH1 mutated brain cancers therapy.

## 4. Experimental section

### 4.1. Chemistry.

All chemicals with the highest purity were obtained from Shanghai Bide Pharmaceutical Technology Co., Ltd. Organic solvents (reagent grade) were dried over anhydrous  $\text{CaCl}_2$  or molecular sieves. Thin-layer chromatography (TLC) was performed on silica gel GF<sub>254</sub> plates (10×10 cm) from Qingdao Haiyang Chemical Plant (Qingdao, Shandong, China). The spots of reactions were visualized by a ZF-1 type ultraviolet analyzer ( $\lambda = 254 \text{ nm}$ ) purchased from Hangzhou David Science and Education Instrument Co. Ltd. Column chromatography silica gel with 100-200 or 200-300 mesh was obtained from Qingdao Ocean Chemical Plant Factory. Flash column chromatography was carried out on 90-150  $\mu\text{m}$  silica gel columns from Qingdao Marine Chemical Inc. Melting points of the targeted compounds were determined on XT-4 melting-point facility from Beijing Tech Instrument Corp.  $^1\text{H}$  NMR and  $^{13}\text{C}$  NMR spectra were recorded on 300MHz or 500MHz and 75 MHz Bruker ACF-300 spectrometers at ambient temperature.  $^1\text{H}$  NMR and  $^{13}\text{C}$  NMR data were indicated with chemical shifts (ppm,  $\delta$ ) referenced to tetramethylsilane (TMS) as an internal standard, splitting patterns (s, singlet; d, doublet; t, triplet; m, multiplet; dd, double of doublets, etc.) and the coupling constant (J) in Hz. Mass spectrometry was performed on an Agilent 1100 Series (Agilent Technologies, Santa Clara, CA, USA), LC/MSD high performance ion trap mass spectrometer and a Mariner ESI-TOF spectrometer. Reverse phase chromatography with a Shimadzu Shim-Pack VP-ODS (150×4.6 mm i.d, 5  $\mu\text{m}$  particle size, Shimadzu Corp., Kyoto, Japan) column and DAD detection were used to determine the purity of all the new compounds. All the detailed data including H NMR,  $^{13}\text{C}$  NMR, HRMS and HPLC purity is shown in the supporting information.

4.1.1. 3-(6-chloropyrazin-2-yl)-4-isopropylloxazolidin-2-one (**I**)

To a solution of 2,6-dichloropyrazine (100 mg, 0.671 mmol) and (S)-4-isopropylloxazolidin-2-one (86.7 mg, 0.671 mmol) in 5 mL DMF was slowly added with a solution of NaH (35 mg, 1.34 mmol) in 1 mL DMF at an ice bath. The mixture was stirred at 0°C for about 2 hours. After the completion of the reaction monitored by TLC, the mixture was added dropwise to ice water. Then the mixture was extracted with EtOAc. The combined EtOAc extracts were washed with brine, dried over anhydrous Na<sub>2</sub>SO<sub>4</sub> and evaporated to afford the white crude product. Purification of the crude product with flash column chromatography (PE : EA = 8:1, v:v) gave 150 mg of **I** as a white solid, yield 92%. <sup>1</sup>H NMR (300 MHz, DMSO-*d*<sub>6</sub>) δ 9.30 (s, 1H), 8.52 (s, 1H), 4.69-4.67 (m, 1H), 4.49-4.46 (m, 2H), 2.38-2.33 (m, 1H), 0.92-0.78 (dd, *J* = 6.0 Hz, *J* = 9.0 Hz, 6H).

4.1.2. (S)-1-([1,1'-biphenyl]-4-yl)ethan-1-amine (**2a**)

To a solution of **1a** (183 mg, 1.50 mmol), (S)-1-(4-bromophenyl)ethan-1-amine (200 mg, 1 mmol), Pd[P(Ph)<sub>3</sub>]<sub>4</sub> (57.8 mg, 0.05 mmol) and 2N K<sub>2</sub>CO<sub>3</sub> solution (1.00 mL, 2.00 mmol) in anhydrous MeCN (12 mL) was purged with N<sub>2</sub> and refluxed for overnight. After the completion of the reaction monitored by TLC, the solvent was removed under vacuum and the crude mixture was dissolved by EtOAc. Then the solution was filtered. The filtrate was washed by water and dried over anhydrous Na<sub>2</sub>SO<sub>4</sub>. After about two hours, the concentrated hydrochloric acid was added dropwise to the solution to adjust pH to 1. The mixture was stirred for 1.5 hours. Then the mixture was washed by water and the combined water layer was added with 5 mol/L NaOH to adjust pH to 10. Finally, the mixture was extracted with CH<sub>2</sub>Cl<sub>2</sub> and the organic layer was removed under vacuum to give the crude product, which can be used for the next step without further purification.

4.1.3. (S)-1-(4'-fluoro-[1,1'-biphenyl]-4-yl)ethan-1-amine (**2b**)

According to the preparation procedure of **2a**, **2b** were prepared as a yellow oil, yield 47.2%. <sup>1</sup>H NMR (300 MHz, DMSO-*d*<sub>6</sub>) δ 7.62 (d, *J* = 7.3 Hz, 2H), 7.55 (t, *J* = 10.0 Hz, 2H), 7.48-7.37 (m, 4H), 7.32 (t, *J* = 7.2 Hz, 1H), 4.01 (q, *J* = 6.4 Hz, 1H), 1.25 (t, *J* = 7.1 Hz, 3H).

#### 4.1.4. (S)-1-(R)ethan-1-amines (**2c-2m**)

According to the preparation procedure of **2a**, **2c-2m** were prepared as a yellow oil.

#### 4.1.5. 3-(6-((1-([1,1'-biphenyl]-4-yl)ethyl)amino)pyrazin-2-yl)-4-isopropylloxazolidin-2-one (**3a**)

To a solution of **2a** (144 mg, 0.73 mmol), **I** (126 mg, 0.52 mmol), tris(dibenzylideneacetone)dipalladium (4.76 mg, 0.0052 mmol), BINAP (13.0 mg, 0.021 mmol) and K<sub>2</sub>CO<sub>3</sub> (100 mg, 0.73 mmol) in anhydrous toluene (12 mL) was purged with N<sub>2</sub> and heated at 90°C for overnight. After the completion of the reaction monitored by TLC, the mixture was added with water and extracted with EtOAc. The EtOAc extracts were washed by saturated brine and dried over anhydrous Na<sub>2</sub>SO<sub>4</sub>. Purification of the crude product with flash column chromatography (PE : EA = 3:1, v:v) gave **3a** as a white solid (100 mg, 38.1%). Mp: 175-178°C. <sup>1</sup>H NMR (300 MHz, CDCl<sub>3</sub>) δ 8.66 (s, 1H), 7.76 (s, 1H), 7.54 (d, *J* = 6.4 Hz, 4H), 7.48-7.29 (m, 5H), 5.20 (s, 1H), 5.02-4.85 (m, 1H), 4.61-4.48 (m, 1H), 4.32 (t, *J* = 8.7 Hz, 1H), 4.25-4.13 (m, 1H), 1.87 (s, 1H), 1.62 (d, *J* = 6.8 Hz, 3H), 0.64 (d, *J* = 6.3 Hz, 6H). <sup>13</sup>C NMR (75 MHz, DMSO-*d*<sub>6</sub>) δ 154.35, 152.41, 144.74, 144.66, 140.13, 138.40, 128.83, 127.32, 127.12, 126.62, 126.46, 125.95, 120.76, 62.87, 57.79, 49.50, 26.93, 23.54, 17.58, 13.68. HRMS (m/z) 403.2131 [M + H]<sup>+</sup>. HPLC purity 98.69 %.

#### 4.1.6. (S)-3-(6-(((S)-1-(4'-fluoro-[1,1'-biphenyl]-4-yl)ethyl)amino)pyrazin-2-yl)-4-isopropylloxazolidin-2-one (**3b**)

According to the preparation procedure of **3a**, **3b** was prepared as a white solid, yield 38.2%. Mp: 174-176°C. <sup>1</sup>H NMR (300 MHz, DMSO-*d*<sub>6</sub>) δ 8.28 (s, 1H), 7.82-7.72 (m, 2H), 7.68-7.59 (m, 2H), 7.55

(d,  $J = 8.2$  Hz, 2H), 7.37 (d,  $J = 8.0$  Hz, 2H), 7.26 (t,  $J = 8.8$  Hz, 2H), 4.99–4.88 (m, 1H), 4.50 (d,  $J = 8.7$  Hz, 1H), 4.34 (t,  $J = 8.8$  Hz, 1H), 4.23 (d,  $J = 8.9$  Hz, 1H), 1.63 (s, 1H), 1.48 (d,  $J = 6.9$  Hz, 3H), 0.56 (d,  $J = 6.9$  Hz, 3H), 0.45 (d,  $J = 6.8$  Hz, 3H).  $^{13}\text{C}$  NMR (75 MHz, DMSO- $d_6$ )  $\delta$  163.29, 154.32, 152.37, 144.71, 144.64, 137.33, 136.53, 128.40, 128.30, 127.28, 126.54, 125.95, 120.75, 115.73, 115.44, 62.84, 57.76, 49.45, 26.91, 23.50, 17.55, 13.66. HRMS ( $m/z$ ) 421.2036 [ $\text{M} + \text{H}$ ] $^+$ . HPLC purity 99.56%.

4.1.7. (S)-3-(6-(((S)-1-(3'-fluoro-[1,1'-biphenyl]-4-yl)ethyl)amino)pyrazin-2-yl)-4-isopropylloxazolidin-2-one (**3c**)

According to the preparation procedure of **3a**, **3c** was prepared as a white solid, yield 39.2%. Mp: 184–186°C.  $^1\text{H}$  NMR (300 MHz, DMSO- $d_6$ )  $\delta$  8.29 (s, 1H), 7.79 (s, 2H), 7.62 (d,  $J = 8.1$  Hz, 2H), 7.49–7.36 (m, 5H), 7.16 (s, 1H), 4.95 (s, 1H), 4.51–4.45 (m, 1H), 4.33 (d,  $J = 9.0$  Hz, 1H), 4.25–4.20 (m, 1H), 1.65–1.60 (m, 1H), 1.48 (d,  $J = 6.9$  Hz, 3H), 0.56 (d,  $J = 6.9$  Hz, 3H), 0.45 (d,  $J = 6.8$  Hz, 3H).  $^{13}\text{C}$  NMR (75 MHz, DMSO- $d_6$ )  $\delta$  164.23, 154.32, 152.36, 145.40, 144.71, 136.91, 130.78, 130.67, 127.28, 126.72, 126.00, 122.47, 120.78, 113.94, 113.66, 113.20, 112.91, 62.84, 57.76, 49.47, 26.91, 23.48, 17.54, 13.65. HRMS ( $m/z$ ) 421.2041 [ $\text{M} + \text{H}$ ] $^+$ . HPLC purity 99.34 %.

4.1.8. (S)-3-(6-(((S)-1-(2'-fluoro-[1,1'-biphenyl]-4-yl)ethyl)amino)pyrazin-2-yl)-4-isopropylloxazolidin-2-one (**3d**)

According to the preparation procedure of **3a**, **3d** was prepared as a white solid, yield 39.1%. Mp: 176–178°C.  $^1\text{H}$  NMR (300MHz, DMSO- $d_6$ )  $\delta$  8.30 (s, 1H), 7.78 (d,  $J = 9.3$  Hz, 2H), 7.47 (d,  $J = 7.1$  Hz, 3H), 7.39 (d,  $J = 8.2$  Hz, 3H), 7.28 (t,  $J = 7.9$  Hz, 2H), 5.10–4.86 (m, 1H), 4.57–4.43 (m, 1H), 4.34 (t,  $J = 8.8$  Hz, 1H), 4.29–4.17 (m, 1H), 1.63 (s, 1H), 1.49 (d,  $J = 6.9$  Hz, 3H), 0.56 (d,  $J = 6.9$  Hz, 3H), 0.46 (d,  $J = 6.8$  Hz, 3H).  $^{13}\text{C}$  NMR (75 MHz, DMSO- $d_6$ )  $\delta$  160.66, 154.32, 152.36, 145.10, 144.73, 133.14,

130.55, 130.50, 129.28, 129.17, 128.70, 128.66, 127.29, 125.58, 124.82, 124.77, 120.71, 116.13, 115.83, 62.85, 57.76, 49.49, 26.90, 23.49, 17.50, 13.61. HRMS (m/z) 421.2033 [M + H]<sup>+</sup>. HPLC purity 99.36 %.

4.1.9. (S)-4-isopropyl-3-(6-(((S)-1-(4'-methoxy-[1,1'-biphenyl]-4-yl)ethyl)amino)pyrazin-2-yl)oxazolidin-2-one (**3e**)

According to the preparation procedure of **3a**, **3e** was prepared as a white solid, yield 45.2%. Mp: 138-141°C. <sup>1</sup>H NMR (300 MHz, DMSO-*d*<sub>6</sub>) δ 8.28 (s, 1H), 7.81–7.71 (m, 2H), 7.58–7.47 (m, 4H), 7.34 (d, *J* = 8.1 Hz, 2H), 7.00 (d, *J* = 8.4 Hz, 2H), 4.92 (d, *J* = 7.2 Hz, 1H), 4.48 (s, 1H), 4.34 (t, *J* = 8.9 Hz, 1H), 4.23 (d, *J* = 9.0 Hz, 1H), 3.78 (s, 3H), 1.64 (s, 1H), 1.48 (d, *J* = 6.8 Hz, 3H), 0.57 (d, *J* = 6.9 Hz, 3H), 0.46 (d, *J* = 6.9 Hz, 3H). <sup>13</sup>C NMR (75 MHz, DMSO-*d*<sub>6</sub>) δ 158.59, 152.38, 144.71, 143.82, 138.04, 131.07, 127.57, 127.48, 127.27, 126.08, 125.86, 120.68, 114.28, 62.83, 57.76, 55.08, 49.44, 26.89, 23.51, 17.56, 13.66. HRMS (m/z) 433.2236 [M + H]<sup>+</sup>. HPLC purity 99.08 %.

4.1.10. (S)-4-isopropyl-3-(6-(((S)-1-(3'-methoxy-[1,1'-biphenyl]-4-yl)ethyl)amino)pyrazin-2-yl)oxazolidin-2-one (**3f**)

According to the preparation procedure of **3a**, **3f** was prepared as a white solid, yield 46.0%. Mp: 170-173°C. <sup>1</sup>H NMR (300 MHz, DMSO-*d*<sub>6</sub>) δ 8.29 (s, 1H), 7.77 (d, *J* = 11.0 Hz, 2H), 7.57 (d, *J* = 8.0 Hz, 2H), 7.35 (t, *J* = 8.7 Hz, 3H), 7.23-7.03 (m, 2H), 6.90 (d, *J* = 8.1 Hz, 1H), 5.07-4.86 (m, 1H), 4.57-4.41 (m, 1H), 4.34 (t, *J* = 8.8 Hz, 1H), 4.25-4.15 (m, 1H), 3.80 (s, 3H), 1.61 (s, 1H), 1.48 (d, *J* = 6.9 Hz, 3H), 0.56 (d, *J* = 6.9 Hz, 3H), 0.45 (d, *J* = 6.8 Hz, 3H). <sup>13</sup>C NMR (75 MHz, DMSO-*d*<sub>6</sub>) δ 159.64, 154.33, 152.38, 144.80, 144.71, 141.63, 138.27, 129.86, 127.29, 126.70, 125.87, 120.75, 118.78, 112.58, 112.12, 62.84, 57.76, 54.99, 49.49, 26.90, 23.52, 17.57, 13.67. HRMS (m/z) 433.2235 [M + H]<sup>+</sup>. HPLC purity 98.80 %.

## 4.1.11. (S)-4-isopropyl-3-(6-(((S)-1-(2'-methoxy-[1,1'-biphenyl]-4-yl)ethyl)amino)pyrazin-2-yl)

oxazolidin-2-one (**3g**)

According to the preparation procedure of **3a**, **3g** was prepared as a white solid, yield 46.3%. Mp: 153-155°C. <sup>1</sup>H NMR (300 MHz, DMSO-*d*<sub>6</sub>) δ 8.31 (s, 1H), 7.83–7.72 (m, 2H), 7.39 (d, *J* = 8.1 Hz, 2H), 7.30 (dd, *J* = 10.4, 4.7 Hz, 3H), 7.25–7.19 (m, 1H), 7.08 (d, *J* = 8.1 Hz, 1H), 7.00 (t, *J* = 7.4 Hz, 1H), 4.96 (p, *J* = 6.9 Hz, 1H), 4.60–4.48 (m, 1H), 4.35 (t, *J* = 8.8 Hz, 1H), 4.24 (dd, *J* = 9.0, 3.4 Hz, 1H), 3.73 (s, 3H), 1.71 (d, *J* = 3.2 Hz, 1H), 1.49 (d, *J* = 6.9 Hz, 3H), 0.61 (d, *J* = 6.9 Hz, 3H), 0.50 (d, *J* = 6.9 Hz, 3H). <sup>13</sup>C NMR (75 MHz, DMSO-*d*<sub>6</sub>) δ 156.06, 154.33, 152.38, 144.75, 143.85, 136.25, 130.16, 129.63, 129.08, 128.57, 127.24, 125.01, 120.65, 120.57, 111.61, 62.86, 57.82, 55.29, 49.46, 26.89, 23.50, 17.52, 13.63. HRMS (*m/z*) 433.2233 [M + H]<sup>+</sup>. HPLC purity 99.72%.

## 4.1.12. (S)-4-isopropyl-3-(6-(((S)-1-(4'-methyl-[1,1'-biphenyl]-4-yl)ethyl)amino)pyrazin-2-yl)

oxazolidin-2-one (**3h**)

According to the preparation procedure of **3a**, **3h** was prepared as a white solid, yield 50.1%. Mp: 165-170°C. <sup>1</sup>H NMR (300 MHz, DMSO-*d*<sub>6</sub>) δ 8.28 (s, 1H), 7.89-7.65 (m, 2H), 7.52 (dd, *J* = 15.6, 8.1 Hz, 4H), 7.35 (d, *J* = 8.1 Hz, 2H), 7.24 (d, *J* = 7.9 Hz, 2H), 4.94 (t, *J* = 6.9 Hz, 1H), 4.61-4.43 (m, 1H), 4.34 (t, *J* = 8.8 Hz, 1H), 4.22 (dd, *J* = 9.0, 3.4 Hz, 1H), 2.32 (s, 3H), 1.63 (s, 1H), 1.48 (d, *J* = 6.9 Hz, 3H), 0.56 (d, *J* = 6.9 Hz, 3H), 0.45 (d, *J* = 6.8 Hz, 3H). <sup>13</sup>C NMR (75 MHz, DMSO-*d*<sub>6</sub>) δ 154.32, 152.39, 144.71, 144.29, 138.28, 137.21, 136.37, 129.40, 127.30, 126.31, 126.24, 125.88, 120.72, 62.83, 57.76, 49.48, 26.88, 23.52, 20.54, 17.55, 13.64. HRMS (*m/z*) 417.2292 [M + H]<sup>+</sup>. HPLC purity 99.18%.

## 4.1.13. (S)-4-isopropyl-3-(6-(((S)-1-(3'-methyl-[1,1'-biphenyl]-4-yl)ethyl)amino)pyrazin-2-yl)

oxazolidin-2-one (**3i**)

According to the preparation procedure of **3a**, **3i** was prepared as a white solid, yield 50.1%. Mp:

145-149°C.  $^1\text{H}$  NMR (300 MHz, DMSO- $d_6$ )  $\delta$  8.29 (s, 1H), 7.84-7.70 (m, 2H), 7.55 (d,  $J = 8.1$  Hz, 2H), 7.35 (dt,  $J = 18.6, 7.6$  Hz, 5H), 7.14 (d,  $J = 7.2$  Hz, 1H), 4.95 (t,  $J = 6.8$  Hz, 1H), 4.56-4.45 (m, 1H), 4.34 (t,  $J = 8.8$  Hz, 1H), 4.23 (dd,  $J = 9.0, 3.4$  Hz, 1H), 2.35 (s, 3H), 1.63 (s, 1H), 1.48 (d,  $J = 6.9$  Hz, 3H), 0.56 (d,  $J = 6.9$  Hz, 3H), 0.45 (d,  $J = 6.8$  Hz, 3H).  $^{13}\text{C}$  NMR (75 MHz, DMSO- $d_6$ )  $\delta$  154.32, 152.38, 144.72, 144.53, 140.07, 138.48, 137.89, 128.69, 127.76, 127.27, 127.09, 126.57, 125.88, 123.57, 120.71, 62.85, 57.77, 49.46, 26.91, 23.51, 21.05, 17.56, 13.67. HRMS (m/z) 417.2293 [M + H] $^+$ . HPLC purity 98.94%.

4.1.14. (S)-4-isopropyl-3-(6-(((S)-1-(2'-methyl-[1,1'-biphenyl]-4-yl)ethyl)amino)pyrazin-2-yl)oxazolidin-2-one (**3j**)

According to the preparation procedure of **3a**, **3j** was prepared as a white solid, yield 49.1%. Mp: 176-179°C.  $^1\text{H}$  NMR (300 MHz, DMSO- $d_6$ )  $\delta$  8.32 (s, 1H), 7.78 (d,  $J = 6.3$  Hz, 2H), 7.44-7.31 (m, 2H), 7.24 (t,  $J = 7.8$  Hz, 5H), 7.14 (d,  $J = 4.7$  Hz, 1H), 5.00 (t,  $J = 6.9$  Hz, 1H), 4.64-4.50 (m, 1H), 4.36 (t,  $J = 8.7$  Hz, 1H), 4.31-4.15 (m, 1H), 2.20 (s, 3H), 1.73 (s, 1H), 1.50 (d,  $J = 6.9$  Hz, 3H), 0.62 (d,  $J = 6.9$  Hz, 3H), 0.51 (d,  $J = 6.8$  Hz, 3H).  $^{13}\text{C}$  NMR (75 MHz, DMSO- $d_6$ )  $\delta$  152.37, 144.77, 144.05, 141.08, 139.32, 134.56, 130.23, 129.36, 128.81, 127.24, 127.08, 125.83, 125.24, 120.50, 62.97, 57.78, 49.34, 27.01, 23.58, 20.06, 17.65, 13.77. HRMS (m/z) 417.2286 [M + H] $^+$ . HPLC purity 98.71 %.

4.1.15. (S)-4-isopropyl-3-(6-(((S)-1-(4'-(trifluoromethyl)-[1,1'-biphenyl]-4-yl)ethyl)amino)pyrazin-2-yl)oxazolidin-2-one (**3k**)

According to the preparation procedure of **3a**, **3k** was prepared as a white solid, yield 53.1%. Mp: 96-98°C.  $^1\text{H}$  NMR (300 MHz, DMSO- $d_6$ )  $\delta$  8.30 (s, 1H), 7.81 (q,  $J = 8.3$  Hz, 6H), 7.66 (d,  $J = 7.6$  Hz, 2H), 7.43 (d,  $J = 7.8$  Hz, 2H), 5.02-4.90 (m, 1H), 4.53-4.42 (m, 1H), 4.34 (t,  $J = 8.7$  Hz, 1H), 4.26-4.18 (m, 1H), 1.59 (s, 1H), 1.50 (d,  $J = 6.8$  Hz, 3H), 0.55 (d,  $J = 6.7$  Hz, 3H), 0.44 (d,  $J = 6.7$  Hz, 3H).  $^{13}\text{C}$

NMR (75 MHz, DMSO- $d_6$ )  $\delta$  154.33, 152.35, 145.87, 144.65, 144.04, 136.67, 127.30, 127.17, 126.96, 126.12, 125.72, 125.67, 120.80, 62.84, 57.74, 49.49, 26.91, 23.48, 17.55, 13.66. HRMS (m/z) 471.2003 [M + H]<sup>+</sup>. HPLC purity 97.79 %.

4.1.16. (S)-4-isopropyl-3-(6-(((S)-1-(4-(naphthalen-2-yl)phenyl)ethyl)amino)pyrazin-2-yl)oxazolidin-2-one (**3l**)

According to the preparation procedure of **3a**, **3l** was prepared as a white solid, yield 52.3%. Mp: 210-214°C. <sup>1</sup>H NMR (500 MHz, CDCl<sub>3</sub>)  $\delta$  8.67 (s, 1H), 7.99 (s, 1H), 7.94–7.84 (m, 3H), 7.68 (dd,  $J$  = 15.2, 9.4 Hz, 4H), 7.56–7.46 (m, 2H), 7.40 (d,  $J$  = 8.0 Hz, 2H), 5.01–4.89 (m, 2H), 4.60–4.51 (m, 1H), 4.32 (t,  $J$  = 8.9 Hz, 1H), 4.20 (dd,  $J$  = 9.0, 3.6 Hz, 1H), 1.88 (dd,  $J$  = 10.6, 6.7 Hz, 1H), 1.63 (d,  $J$  = 6.5 Hz, 3H), 0.64 (t,  $J$  = 6.1 Hz, 6H). <sup>13</sup>C NMR (75 MHz, DMSO- $d_6$ )  $\delta$  154.33, 152.40, 144.82, 138.12, 137.40, 133.28, 132.07, 128.35, 128.03, 127.39, 127.32, 126.87, 126.30, 126.03, 125.92, 124.96, 124.82, 120.78, 62.84, 57.78, 49.52, 28.91, 26.93, 23.53, 17.59, 13.67. HRMS (m/z) 453.2290 [M + H]<sup>+</sup>. HPLC purity 99.01 %.

4.1.17. (S)-3-(6-(((S)-1-(4-(3,5-dimethylisoxazol-4-yl)phenyl)ethyl)amino)pyrazin-2-yl)-4-isopropyl-oxazolidin-2-one (**3m**)

According to the preparation procedure of **3a**, **3m** was prepared as a white solid, yield 49.8%. Mp: 175-178°C. <sup>1</sup>H NMR (500 MHz, CDCl<sub>3</sub>)  $\delta$  8.67 (d,  $J$  = 13.4 Hz, 1H), 7.67 (s, 1H), 7.37 (d,  $J$  = 8.0 Hz, 2H), 7.21 (d,  $J$  = 8.0 Hz, 2H), 4.96–4.88 (m, 2H), 4.61–4.54 (m, 1H), 4.33 (t,  $J$  = 8.9 Hz, 1H), 4.23 (dd,  $J$  = 9.0, 3.5 Hz, 1H), 2.39 (s, 3H), 2.26 (s, 3H), 1.99 (dd,  $J$  = 10.8, 6.7 Hz, 1H), 1.60 (d,  $J$  = 6.7 Hz, 3H), 0.68 (d,  $J$  = 6.6 Hz, 6H). <sup>13</sup>C NMR (75 MHz, DMSO- $d_6$ )  $\delta$  164.75, 157.98, 154.31, 152.32, 144.71, 128.69, 127.87, 127.23, 125.85, 120.59, 115.69, 62.96, 57.75, 49.36, 27.05, 23.50, 17.57, 13.78, 11.19, 10.37. HRMS (m/z) 422.2190 [M + H]<sup>+</sup>. HPLC purity 98.22 %.

## 4.2. Biological Assays.

The relevant biological assays were performed according to the previous methods [26].

### 4.2.1. IDH1 mutant generation and cloning.

IDH1 mutants were generated using the site directed mutagenesis and validated as described before [27]. The pDONR221 clones were used for all further LR-reactions into the described destination vectors. LR-reactions were performed following the manufacturers protocol (Invitrogen, Carlsbad, USA).

### 4.2.2. Cell culture.

Human embryonic kidney cell line HEK293 was obtained from the ATCC and cultured under standard culture conditions (37 °C, 5% CO<sub>2</sub>) in DMEM medium with 1% penicillin and streptomycin and 10% fetal calf serum (all obtained from Gibco® Invitrogen, Carlsbad, USA). To generate HEK293 cell lines which express IDH1 WT and mutant proteins, we used cDNAs in pMXs-GW-IRES-BsdR transfected with FuGene®HD (Promega, Madison, USA). Cells were subsequently put under selection pressure, by adding 4 mg mL<sup>-1</sup> Blasticidine S (Sigma Aldrich, St. Louis, USA).

### 4.2.3. *In vitro* 2-HG reduction.

$2 \times 10^5$  cells per well in 1 mL of the medium were seeded in a 12-well plate and treated with an appropriate dilution of the compound in DMSO. DMSO was used as solvent control (final concentration 0.01%). The cells were incubated at standard conditions (37 °C, 5% CO<sub>2</sub>) for 72 h. There after supernatant was removed and subsequently analyzed with 2-HG assay. The cells were washed with PBS (Gibco® Invitrogen, Carlsbad, USA) and treated with 150 µL NP-40 lysis buffer; 50 mM Tris-HCl, pH 8.0 (Sigma Aldrich, St.Louis, USA), 150 mM NaCl (Sigma Aldrich, St. Louis, USA), 0.1% NP-40

(USBiologicals, Salem, MA, USA) and complete protease inhibitor (Roche, Basel, Switzerland). This suspension was recovered from the plate and lysate was progressed in three freeze & thaw cycles with liquid nitrogen. There after the lysate was centrifuged at 16.1g for 15 min, the supernatant was transferred to another tube and protein concentration of it was determined with BCA assay kit (Thermo Fisher Scientific, Waltham, USA) following the manufacturer's protocol.

#### 4.2.4. 2-HG assay.

The 2-HG assay has been described previously [28]. In brief, probe material was treated with a deproteinization kit (Biovision, Mountain View, CA, USA). Supernatants were then collected and stored at  $-20^{\circ}\text{C}$ . The total enzymatic reaction volume was 100  $\mu\text{L}$ . Ten milliliter of assay solution was freshly prepared for each 96-well plate subjected to D2HG assay. The assay solution contained 100 mM HEPES pH 8.0, 100  $\mu\text{M}$   $\text{NAD}^{+}$  (Applichem, Darmstadt, Germany), 0.1  $\mu\text{g}$  HGDH, 5  $\mu\text{M}$  resazurin (Applichem, Darmstadt, Germany) and 0.01  $\text{U mL}^{-1}$  diaphorase (0.01  $\text{U mL}^{-1}$ ; MP Biomedical, Irvine, USA). Immediately before use, 25  $\mu\text{L}$  sample volume was added to 75  $\mu\text{L}$  of assay solution and incubated at room temperature for 30 min in black 96-well plates (Thermo Fisher Scientific, Waltham, USA) in the dark. Fluorometric detection was performed in triplicate with 25  $\mu\text{L}$  deproteinized sample being analyzed in each reaction with excitation at  $540 \pm 10$  nm and emission of  $580 \pm 10$  nm (FLUOstar Omega, BMG Labtech, Offenburg, Germany).

#### 4.2.5. Cell viability assay.

HEK-293T cells carrying pMXs-IDH1wtIRES-BsdRs were seeded in white opaque 96-well plates (Falcon®, Corning, New York, USA) at a density of 10 000 cells per well. Subsequently they were treated with compound at the depicted concentration and incubated for 72 h. There after the cell viability was analyzed using CellTiterGlo (Promega, Madison, USA) following the manufacturers protocol.

### 4.3. Molecular docking studies

#### 4.3.1. Preparation of protein structure

The X-ray structure of IDH1-R132H homodimer in a complex with **SYC-435** (PDB code **4XRX**) and **IDH889** (PDB code **5TQH**) were obtained from Protein Data Bank and were reserved for docking-based studies. All water molecules were cleaned utilizing the Prepare Protein utility in Maestro 14.0. Briefly, all hydrogen atoms were added properly to the complexes and hydrogen bond formations were well maximized by the optimization of key residues.

#### 4.3.2. Preparing the ligand database

Compounds were sketched in ChemBioDraw14.0 and converted into 3D structures followed by a local minimization using MMFF force field. The resulting structures were used for the following docking simulations.

#### 4.3.3. Docking procedure

First, protein's geometry was optimized utilizing a fast Dreiding-like force field. And the targeted protein was completely checked by the "Clean Geometry" toolkit of DS 3.0. Then, 10 replicas for each described compound were produced as a spherical scope with a diameter of 18 Å and centered on IDH1-R132H inhibitor adduct. Besides, random conformation was limited as 10, simulated annealing methods were set to true and other parameters were retained by default. Finally, ten best conformations were saved for further analysis and molecular docking.

### 4.4. PAMPA-BBB assays.

The permeability of the compounds was determined by a PAMPA-BBB assay [29]. The tested drugs (**3g**, **Desipramine** as a positive control and **Atenolol** as a negative control) were dissolved in DMSO to

5 mg/ml stock solutions, and 10  $\mu$ L sample mother liquor was diluted with PBS into secondary mother liquor (final concentration: 25  $\mu$ g/ml). All solutions were filtered through a filter. Then 300  $\mu$ L secondary mother liquors were added into every donor well. The porcine polar brain lipid (PBL) was dissolved in twelve burns (20 mg/mL) and 4  $\mu$ L of the mixture was added dropwise to simulate the biofilm on the lipophilic membrane of the recipient wells. 150  $\mu$ L PBS buffer was taken to the acceptor well. In addition, the phospholipid membrane was carefully contacted with the donor fluid. Then the formation of sandwich structure was formed that the donor plate containing the test drugs was in the bottom, the artificial phospholipid membrane was in the middle, acceptor plate was in the top. The “sandwich” was left for 18h at room temperature. After incubation, the concentration of the test drugs in the reference solution and the acceptor plate was determined using a UV plate reader. Finally, the effective transmittance ( $P_e$ ) of the compounds was calculated by a formula.

$$P_e = -\frac{V_{dn}V_{ac}}{st(V_{dn} + V_{ac})} \ln\left\{1 - \frac{[drug]_{ac}}{[drug]_{ref}}\right\}$$

### Supplementary data

Supplementary data associated with this article can be found, in the online version, at <http://>

### Author Information

Corresponding Authors

\*For X. Zha: phone, +86-25-86185474; fax, +86-25-86185474; e-mail, xmzha@cpu.edu;

\*For A. von Deimling: phone, +49-6221-56-4650; fax: +49-6221-56-4655; e-mail,

andreas.vondeimling@med.uni-heidelberg.de;

# These authors contributed equally to this work.

## Notes

Prof. Andreas von Deimling and Dr. Stefan Pusch are patent holders for the enzymatic 2-HG detection assay. All other authors declare no competing financial interest.

## Acknowledgments

This work was supported by the Natural Science Foundation of Jiangsu Province (BK20161458), “Six Talent Peaks” Project of Jiangsu Province (2016-YY-042) and Postgraduate Research & Practice Innovation Program of Jiangsu Province (KYCX17\_0721).

## Abbreviations

IDH, Isocitrate dehydrogenase; TCA, the tricarboxylic acid;  $\alpha$ -KG,  $\alpha$ -Ketoglutaric acid; D2HG, D-2-Hydroxyglutaric acid; mIDH1, Mutant IDH1; mIDH2, Mutant IDH2; R132H, Arg132 mutation to His; R132C, Arg132 mutation to Cys; R140Q, Arg140 mutation to Gln; WT, wild type; BBB, Blood Brain Barrier;

## References

[1] J. Chen, J. Yang, P. Cao, The Evolving Landscape in the Development of Isocitrate Dehydrogenase Mutant Inhibitors, *Mini-Rev. Med. Chem.* 16 (2016) 1344-1358.

- [2] L. Dang, S.M. Su, Isocitrate Dehydrogenase Mutation and (R)-2-Hydroxyglutarate: From Basic Discovery to Therapeutics Development, *Annu. Rev. Biochem.* 2017.
- [3] Z.J. Reitman, H. Yan, Isocitrate Dehydrogenase 1 and 2 Mutations in Cancer: Alterations at a Crossroads of Cellular Metabolism, *JNCI J. Natl. Cancer Inst.* 102 (2010) 932–941.
- [4] L. Dang, K. Yen, E. C. Attar, IDH mutations in cancer and progress toward development of targeted therapeutics, *Ann Oncol.* 27 (2016) 599-608.
- [5] P.L. Sulkowski, C.D. Corso, N.D. Robinson, et al, 2-Hydroxyglutarate produced by neomorphic IDH mutations suppresses homologous recombination and induces PARP inhibitor sensitivity, *Sci. Transl. Med.* 9 (2017) 1-15.
- [6] C. Hartmann, J. Meyer, J. Balss, D. Capper, W. Mueller, A. Christians, J. Felsberg, M. Wolter, C. Mawrin, W. Wick, M. Weller, C. Herold-Mende, A. Unterberg, J.W.M. Jeuken, P. Wesseling, G. Reifenberger, A. von Deimling, Type and frequency of IDH1 and IDH2 mutations are related to astrocytic and oligodendroglial differentiation and age: a study of 1,010 diffuse gliomas, *Acta Neuropathol.* 118 (2009) 469–474.
- [7] L. Dang, D.W. White, S. Gross, B.D. Bennett, M.A. Bittinger, E.M. Driggers, V.R. Fantin, H.G. Jang, S. Jin, M.C. Keenan, K.M. Marks, R.M. Prins, P.S. Ward, K.E. Yen, L.M. Liau, J.D. Rabinowitz, L.C. Cantley, C.B. Thompson, M.G. Vander Heiden, S.M. Su, Cancer associated IDH1 mutations produce 2-hydroxyglutarate, *Nature.* 462 (2009) 739-744.
- [8] E. Baader, G. Tschank, K.H. Baringhaus, et al, Inhibition of prolyl 4-hydroxylase by oxalyl amino acid derivatives in vitro, in isolated microsomes and in embryonic chicken tissues, *Biochem. J.* 300 (1994) 525.

- [9] D. Ye, Y. Xiong, K.L. Guan, The mechanisms of IDH mutations in tumorigenesis, *Cell Res.* 22 (2012) 1102-1104.
- [10] J. A. Losman, R. E. Looper, P. Koivunen, S. Lee, R.K. Schneider, C. McMahon, G. S. Cowley, D.E. Root, B.L. Ebert, W.G.Jr. Kaelin, (R)-2-hydroxyglutarate is sufficient to promote leukemogenesis and its effects are reversible, *Science.* 339 (2013) 1621-1625.
- [11] E. Hansen, C. Quivoron, K. Straley, R.M. Lemieux, J. Popovici-Muller, H. Sadrzadeh, A.T. Fathi, C. Gliser, M. David, V. Saada, J.B. Micol, O. Bernard, M. Dorsch, H. Yang, M. Su, S. Agresta, S. de Botton, V. Penard-Lacronique, K. Yen, AG-120, an Oral, Selective, First-in-Class, Potent Inhibitor of Mutant IDH1, Reduces Intracellular 2HG and Induces Cellular Differentiation in TF-1 R132H Cells and Primary Human IDH1 Mutant AML Patient Samples Treated Ex Vivo, *Blood.* 124 (2014) 3734.
- [12] Agios Announces First Patient Dosed with AG-881 in Phase 1 Study in Patients with Advanced Solid Tumors with an IDH Mutation, Agios Pharmaceuticals Press Release. **2015**.
- [13] B. Zheng, Y. Yao, Z. Liu, L. Deng, J. L. Anglin, H. Jiang, B.V.V. Prasad, Y. Song, Crystallographic investigation and selective inhibition of mutant isocitrate dehydrogenase, *Med. Chem. Lett.* 4 (2013) 542–546.
- [14] U.C. Okoye-Okafor, B. Bartholdy, J. Cartier, E.N. Gao, B. Pietrak, A. R. Rendina, C. Rominger, C. Quinn, A. Smallwood, K.J. Wiggall, A.J. Reif, S.J. Schmidt, H. Qi, H. Zhao, G. Joberty, M. Faelth-Savitski, M. Bantscheff, G. Drewes, C. Duraiswami, P. Brady, A. Groy, S.R. Narayanagari, I. Antony-Debre, K. Mitchell, H.R. Wang, Y.R. Kao, M. Christopeit, L. Carvajal, L. Barreyro, E. Paietta, H. Makishima, B. Will, N. Concha, N.D. Adams, B. Schwartz, M.T. McCabe, J. Maciejewski, A. Verma, U. Steidl, New IDH1 mutant inhibitors for treatment of acute myeloid leukemia, *Nat. Chem. Biol.* 11 (2015) 878-886.

- [15] B. Yang, C. Zhong, Y. Peng, Z. Lai, J. Ding, Molecular mechanisms of “off-on switch” of activities of human IDH1 by tumor-associated mutation R132H, *Cell. Res.* 20 (2010) 1188-1200.
- [16] G. Deng, J. Shen, M. Yin, J. McManus, M. Mathieu, P. Gee, T. He, C. Shi, O. Bedel, L.R. McLean, F. Le-Strat, Y. Zhang, J.P. Marquette, Q. Gao, B. Zhang, A. Rak, D. Hoffmann, E. Rooney, A. Vassort, W. Englaro, Y. Li, V. Patel, F. Adrian, S. Gross, D. Wiederschain, H. Cheng, S. Licht, Selective inhibition of mutant isocitrate dehydrogenase 1 (IDH1) via disruption of a metal binding network by an allosteric small molecule, *J. Biol. Chem.* 290 (2015) 762-774.
- [17] D. Rohle, J. Popovici-Muller, N. Palaskas, S. Turcan, C. Grommes, C. Campos, J. Tsoi, O. Clark, B. Oldrini, E. Komisopoulou, K. Kunii, A. Pedraza, S. Schalm, L. Silverman, A. Miller, F. Wang, H. Yang, Y. Chen, A. Kernytsky, M.K. Rosenblum, W. Liu, S.A. Biller, S.M. Su, C.W. Brennan, T.A. Chan, T.G. Graeber, K.E. Yen, I. K. Mellinghoff, An inhibitor of mutant IDH1 delays growth and promotes differentiation of glioma cells, *Science.* 340 (2013) 626–630.
- [18] L. Li, A.C. Paz, B.A. Wilky, B. Johnson, K. Galoian, A. Rosenberg, G. Hu, G. Tinoco, O. Bodamer, J.C. Trent, Treatment with a Small Molecule Mutant IDH1 Inhibitor Suppresses Tumorigenic Activity and Decreases Production of the Oncometabolite 2-Hydroxyglutarate in Human Chondrosarcoma Cells, *PLoS One.* 10 (2015) e0133813.
- [19] S. Pusch, S. Krausert, V. Fischer, J. Balss, M. Ott, D. Schrimpf, D. Capper, F. Sahm, J. Eisel, A.C. Beck, M. Jugold, V. Eichwald, S. Kaulfuss, O. Panknin, H. Rehwinkel, K. Zimmermann, R.C. Hillig, J. Guenther, L. Toschi, R. Neuhaus, A. Haegbart, H. Hess-Stumpp, M. Bauser, W. Wick, A. Unterberg, C. Herold-Mende, M. Platten, A. von Deimling, Pan-mutant IDH1 inhibitor BAY 1436032 for effective treatment of IDH1 mutant astrocytoma in vivo, *Acta Neuropathol.* 133 (2017) 629-644.

- [20] A. Chaturvedi, L. Herbst, S. Pusch, L. Klett, R. Goparaju, D. Stichel, S. Kaulfuss, O. Panknin, K. Zimmermann, L. Toshi, R. Neuhaus, A. Haegebarth, H. Rehwinkel, H. Hess-Stumpp, M. Bauser, T. Bochtler, E.A. Struys, A. Sharma, A. Bakkali, R. Geffers, M.M. Araujo-Cruz, F. Thol, R. Gabdoulline, A. Ganser, A.D. Ho, A. von Deimling, K. Rippe, M. Heuser, A. Krämer, Pan-mutant-IDH1 inhibitor BAY1436032 is highly effective against human IDH1 mutant acute myeloid leukemia in vivo, *Leukemia*. (2017) 1-9.
- [21] M. Heuser, L. Herbst, S. Pusch, L. Klett, R. Goparaju, D. Stichel, S. Kaulfuss, O. Panknin, K. Zimmermann, L. Toschi, R. Neuhaus, A. Haegebarth, H. Rehwinkel, H. Hess-Stumpp, M. Bauser, T. Bochtler, E.A. Struys, A. Sharma, A. Abdellatif, R. Ceffer, M.M.A. Gruz, F. Thol, R. Gaboulline, A. Ganser, A.D. Ho, A. von Deimling, K. Rippe, A. Chaturvedi, A. Kraemer, Pan-Mutant-IDH1 Inhibitor Bay-1436032 Is Highly Effective Against Human IDH1 Mutant Acute Myeloid Leukemia In Vivo, *Blood*. 128 (2016) 745.
- [22] J.M. Law, S.C. Stark, L. Ke, et al, Discovery of 8-Membered Ring Sulfonamides as Inhibitors of Oncogenic Mutant Isocitrate Dehydrogenase 1, *Med. Chem. Lett.* 7 (2016) 944-949.
- [23] S. Jones, J. Ahmet, K. Ayton, et al, Discovery and Optimization of Allosteric Inhibitors of Mutant Isocitrate Dehydrogenase 1 (R132H IDH1) Displaying Activity in Human Acute Myeloid Leukemia Cells, *J. Med. Chem.* 59 (2016) 11120-11137.
- [24] T.R. Caferro, Z. Chen, Y.S. Cho, et al, 3-pyrimidin-4-yl-oxazolidin-2-ones as inhibitors of mutant IDH: WO 2013046136 (A1) [P]. 2013.
- [25] J.R. Levell, T. Caferro, G. Chenail, et al, Optimization of 3-Pyrimidin-4-yl-oxazolidin-2-ones as Allosteric and Mutant Specific Inhibitors of IDH1, *Med. Chem. Lett.* 8 (2016) 151-156.

- [26] F. Zou, S. Pusch, J. Eisel, T. Ma, Q. Zhu, D. Deng, Y. Gu, Y. Xu, A. von Deimling, X. Zha, Identification of a novel selective inhibitor of mutant isocitrate dehydrogenase 1 at allosteric site by docking-based virtual screening, *RSC Adv.* 6 (2016) 96735–96742.
- [27] S. Pusch, L. Schweizer, A.C. Beck, J.M. Lehmler, S. Weissert, J. Balss, A.K. Miller, A. von Deimling, D-2-Hydroxyglutarate producing neo-enzymatic activity inversely correlates with frequency of the type of isocitrate dehydrogenase 1 mutations found in glioma, *Acta Neuropathol. Commun.* 2 (2014) 19.
- [28] J. Balss, S. Pusch, A.C. Beck, C. Herold-Mende, A. Krämer, C. Thiede, W. Buckel, C.D. Langhans, J.G. Okun, A. von Deimling, Enzymatic assay for quantitative analysis of (d)-2-hydroxyglutarate, *Acta Neuropathol.* 124 (2012) 883–891.
- [29] L. Di, E.H. Kerns, K. Fan, O.J. McConnell, G.T. Carter, High throughput artificial membrane permeability assay for blood–brain barrier, *Eur. J. Med. Chem.* 38 (2003) 223–232.

#### Highlights

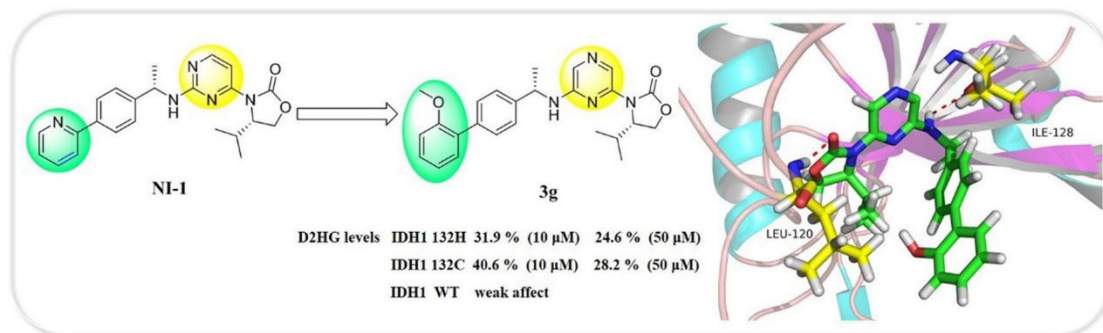
- Synthesis of novel selective mIDH1 inhibitors with 3-pyrazine-4-yl-oxazolidin-2-ones scaffold.
- **3g** shows potent inhibition against IDH1-132H and IDH1-132C as well as high selectivity over

IDH1-WT.

- **3g** can penetrate the blood-brain barrier (BBB).
- **3g** might be a lead compound deserved further structural optimization.

ACCEPTED MANUSCRIPT

Graphic Abstract:



ACCEPTED MANUSCRIPT